

# Krill (*Euphausia superba*) distribution contracts southward during rapid regional warming

Angus Atkinson\*<sup>§1</sup> and Simeon L. Hill<sup>§2</sup>,

Evgeny A. Pakhomov<sup>3,4,5</sup>, Volker Siegel<sup>6</sup>, Christian S. Reiss<sup>7</sup>, Valerie J. Loeb<sup>8</sup>,  
Deborah K. Steinberg<sup>9</sup>, Katrin Schmidt<sup>10</sup>, Geraint A. Tarling<sup>2</sup> Laura Gerrish<sup>2</sup>,  
Sévrine F. Saille<sup>1</sup>

\*Corresponding author

§These joint first authors contributed equally to this work

<sup>1</sup>Plymouth Marine Laboratory, Prospect Place, The Hoe, Plymouth PL1 3DH, UK

<sup>2</sup> British Antarctic Survey, High Cross, Madingley Rd, Cambridge CB3 0ET, UK

<sup>3</sup>Department of Earth, Ocean & Atmospheric Sciences (EOAS), University of British Columbia,  
Vancouver, BC, V6T 1Z4, Canada

<sup>4</sup>Institute for the Oceans and Fisheries, University of British Columbia, 2202 Main Mall,  
Vancouver, BC V6T 1Z4 Canada

<sup>5</sup>Hakai Institute, PO Box 309, Heriot Bay, BC V0P 1H0 Canada

<sup>6</sup>Thuenen Institute of Sea Fisheries, Herwigstr. 31, 27572 Bremerhaven, Germany

<sup>7</sup>Antarctic Ecosystem Research Division, South West Fisheries Science Centre, NOAA Fisheries,  
8901 La Jolla Shores Dr RM333, La Jolla CA 92037, USA

<sup>8</sup>Moss Landing Marine Laboratories, 8272 Moss Landing Road, Moss Landing, CA95039, USA

<sup>9</sup>Virginia Institute of Marine Science, College of William & Mary, Gloucester Point, VA 23062, USA

<sup>10</sup>School of Geography, Earth and Environmental Sciences, University of Plymouth, Drake Circus,  
Plymouth, UK

45           **High latitude ecosystems are among the fastest warming on the planet<sup>1</sup>. Polar**  
46 **species may be sensitive to warming and ice loss, but data are scarce and evidence is**  
47 **conflicting<sup>2-4</sup>. Here we show that, within their main population centre in the southwest**  
48 **Atlantic sector, the distribution of *Euphausia superba* (hereafter “krill”) has contracted**  
49 **southward over the last 90 years. Near their northern limit, densities have declined**  
50 **sharply and the population has become more concentrated towards the Antarctic**  
51 **shelves. A concomitant increase in mean body length reflects reduced recruitment of**  
52 **juvenile krill. We found evidence for environmental controls on recruitment, including**  
53 **reduced density of juveniles following positive anomalies of the Southern Annular Mode**  
54 **(SAM). Such anomalies are associated with warm, windy and cloudy weather and**  
55 **reduced sea ice, all of which may hinder egg production and survival of larval krill<sup>5</sup>.**  
56 **Conversely, the total population density has declined less steeply than the density of**  
57 **recruits, suggesting reduced mortality rates of older krill. The changing distribution is**  
58 **already perturbing the krill-centred food web<sup>6</sup> and may affect biogeochemical cycling<sup>7,8</sup>.**  
59 **Rapid climate change, with associated non-linear adjustments in the roles of keystone**  
60 **species, poses challenges for the management of valuable polar ecosystems<sup>3</sup>.**

61           The pelagic food webs at both poles comprise iconic species, have important  
62 biogeochemical functions<sup>1</sup> and are commercially exploited, prompting concern over how they  
63 will respond to future climate change<sup>2,3</sup>. At the foundation of these food webs are large, lipid-rich  
64 zooplankton species (e.g. euphausiids, copepods and amphipods), which may be particularly  
65 sensitive to warming, given their narrow temperature tolerance and ice-associated life cycles<sup>1-3,9</sup>.  
66 Poleward shifts in species’ distributions are a major response to climatic warming<sup>10</sup>. These shifts  
67 have been observed at both poles but they are highly variable between species, since other  
68 compensation mechanisms are possible<sup>3,4,10</sup>. Long-term projections are particularly uncertain at  
69 the poles because we have so few data on the spatial-temporal context of past changes<sup>2,4</sup>.

70           With its “keystone” role in the food web, Antarctic krill is one of the few polar species with  
71 spatially extensive sampling that spans the last 90 years<sup>11</sup>. The SW Atlantic sector (20°-80°W),  
72 which holds >50% of the circumpolar krill stock<sup>12</sup>, has also warmed rapidly over this time<sup>13</sup>. This  
73 provides an excellent opportunity to understand how a cold water stenotherm responds to rapid  
74 environmental change. Within the multinational KRILLBASE project (see Methods) we rescued  
75 and compiled all available krill net catch data spanning 1926-2016 into two large databases: one  
76 contains their numerical density (numbers of post-larval krill m<sup>-2</sup>), the other includes length  
77 frequency, sex and maturity stage data.

78           During the 1920s and 1930s the highest krill densities were centred in the northern part  
79 of the sector (**Fig. 1a**). Since then this distribution has contracted southward and became  
80 centred more strongly over Antarctic continental shelves. Most of this contraction seems to have  
81 occurred since the 1970s, prior to which high densities were maintained in the South Georgia

82 area. The overall southward contraction across 90 years was ~440 km, manifested as a major  
83 decrease in mean density in the north and a modest decrease in the south (**Fig 1a**).

84 The data available for the SW Atlantic sector since the mid-1970s, including near-  
85 continuous krill time series and multiple indices of environmental variability, are amenable to  
86 further analysis using mixed models (**Table 1**) to detect systematic change over time. In addition  
87 to standardisation for net type, sampling depth, time of day and time of year, our analysis  
88 accounted for the effects of uneven data coverage and known covariates of krill abundance  
89 including latitude and bathymetry<sup>12</sup>. It also ameliorated the effects of variance inhomogeneity  
90 and temporal autocorrelation, and used de-trending to avoid spurious correlation (see Methods).  
91 The data analysed in each model included up to 12 spatio-temporal averages per austral  
92 summer season. **Figs 1a, 2 and 3** illustrate these statistically robust results with simpler models  
93 fitted to annual averages. The mixed models show a strongly negative time trend in krill density  
94 north of 60°S and a weaker trend further south (**Table 1**, see **Fig 1b**). Indeed, density trends at  
95 the highest latitudes sampled (south of 65°S) were neutral or positive (**Fig 2a**). The overall trend  
96 was also apparent in independent subsets of the data based on net size (**Supplementary Table**  
97 **1**), and the stronger negative trends north of 60°S are also apparent in encounter-probability  
98 data (**Supplementary Fig. 1**)

99 There was also a long-term, spatially coherent trend in the separate mean krill length  
100 dataset (**Fig 2b, Fig. 3a, Supplementary Fig. 2**). This equates to an increase of 6mm between  
101 the 1970s and the present, equivalent to a roughly 75% increase in mean individual body mass.  
102 This is opposite in direction to the more common finding of reduced mean body size across the  
103 life-stages in response to warming<sup>14</sup>, and indicates additional changes in demographic  
104 structure. Given the counteracting effects of decreasing numbers and increasing individual  
105 mass, the substantial (70%) decrease in numerical density over 20 years spanning the 1976-  
106 1996 and 1996-2016 eras equates to a smaller (59%) decline in biomass density. In addition to  
107 the opposing long-term trends, length also varied with density on an inter-annual scale, such  
108 that low density years were characterised by a higher than average mean length (**Fig. 3b, Table**  
109 **1**).

110 Previous studies have identified various potential environmental drivers of krill population  
111 dynamics<sup>5,11,15-18</sup>. The clearest environmental covariate of krill density that we found was the  
112 Southern Annular Mode (SAM) (**Fig. 3c**), which is also related to mean length and recruit  
113 density (**Fig. 3d, Table 1**). The SAM is an index of hemisphere-scale atmospheric circulation  
114 which is linked to finer-scale environmental conditions that might influence krill population  
115 dynamics more directly, most likely by affecting the recruitment of small (<30mm) krill to the  
116 population each year<sup>3,5</sup>. Summers of strong recruitment tend to follow periods with negative  
117 SAM anomalies. Sequential years of poor recruitment are periodically boosted by a year or two  
118 of good recruitment where many small krill swell the numbers but depress the average size<sup>5,15,16</sup>.

119 This explains the negative relationship between krill density and mean length (**Table 1**)  
120 illustrated in **Fig. 3b**.

121 Over the last 40 years, recruitment has declined sharply (**Fig. 2c, Extended data Fig.**  
122 **1a, Table 1**) and indeed significantly more abruptly than the decline in total krill density  
123 (**Extended Data Fig. 1b**). This is coincident with an ongoing trend towards increasingly positive  
124 SAM anomalies (**Fig 3 c**) which indicate the southward influence of storm tracks across the SW  
125 Atlantic sector, low pressure, warmer, cloudier and windier conditions and reduced sea ice<sup>5,18-20</sup>.  
126 Such conditions negatively affect adult feeding, impacting early spawning in spring, early larvae  
127 in summer and later larval stages which may need early-forming, complex and well illuminated  
128 marginal sea ice to promote survival<sup>17</sup>. The exact mechanisms are likely to vary with latitude. For  
129 example, increasing summer temperatures at their northern limit present a physiological  
130 challenge for this stenothermal species<sup>9</sup>, where a strong link between climate, temperature  
131 anomalies and krill recruit biomass has also been identified<sup>18</sup>. Further south, near the tip of the  
132 Antarctic Peninsula, the biomass and quality of phytoplankton food have also declined<sup>21</sup>. In  
133 contrast, at the southern part of the Western Antarctic Peninsula, the loss of permanent sea ice  
134 and increases in phytoplankton biomass<sup>20</sup> are associated with a more stable or even increasing  
135 krill density<sup>5,16</sup> (**Fig. 2a**).

136 Suggestions that krill density has declined within the SW Atlantic sector<sup>11,15</sup> have major  
137 ramifications and so have received some debate<sup>3,16,22</sup>. Indeed a recent paper, which analyses  
138 a more limited subset of our database<sup>23</sup>, argues that previous evidence of a decline<sup>11</sup> “is a  
139 consequence of not considering interactions between krill density and unbalanced sampling in  
140 time and space in the data, and not accounting for the different net-types used.” We agree  
141 with these authors<sup>23</sup> that analyses of this complex database require care, and our study  
142 considered each of the issues they identify. The contrast between their<sup>23</sup> conclusions and ours  
143 instead reflects three major differences in approach. First, we followed established practice of  
144 log transforming annual means across spatial units. Conversely, they<sup>23</sup> log transformed at the  
145 level of individual records, down-weighting the influence of the high swarm densities which are  
146 a critical feature of krill distribution<sup>12</sup>. This substantially underestimates the mean and variance  
147 in krill density (their<sup>23</sup> Figs 1, 3) compared to previous studies<sup>12</sup>. Second, we excluded  
148 negatively biased data resulting from sampling in winter or at depths greater than 200m while  
149 they<sup>23</sup> did not. Third, while we used statistical hypothesis testing to assess the probability that  
150 the detected decline is a false trend (type I error, indicated by our P values), they did not  
151 quantify the probability of failing to find a real trend (type II error). Overall, we consider that our  
152 findings provide a more robust picture of the spatial pattern of krill density time trends within  
153 the SW Atlantic sector.

154 Notwithstanding differences in the way that krill density data may be screened and  
155 analysed, the length frequency database provides independent evidence that krill dynamics

156 have changed fundamentally. The coherent inter-relationships among krill density, mean length  
157 and SAM also provide a plausible driving mechanism. The spatial coherence in these changes  
158 supports the concept of a large and connected marine ecosystem linked by advection<sup>18,24</sup>.  
159 Reduced birth weights of fur seals at South Georgia<sup>6</sup> is suggestive of major changes in the krill-  
160 based food web in the northern part of krill's range. Likewise, in the far south, observations of  
161 more stable krill densities and recruitment<sup>5,16</sup> align with our conclusion that the distribution of krill  
162 is contracting southward.

163 Polar food webs are structured both by top-down and bottom-up effects, but their  
164 relative roles are debated<sup>1,2,22</sup>. Several strands of evidence point to climatic change as a major  
165 driver of krill dynamics in this sector. First, in the Indian sector of the Southern Ocean, where  
166 sea ice and temperature have been more relatively stable over the last 50 years<sup>19</sup>, there was no  
167 evidence for the basin-scale decline in krill stocks that is observed in the rapidly warming SW  
168 Atlantic sector<sup>11</sup>. Second, within the SW Atlantic sector the gradation from a steep decline in  
169 density at lower latitudes towards an increase in the south concurs with observed and projected  
170 poleward distribution shifts under warming<sup>2,3,10</sup>. These changes cannot be explained by any  
171 known changes in the suite of krill predators. The relationships between de-trended SAM and  
172 krill population variables are both significant and coherent but other drivers and time-lags,  
173 unresolvable at our scale of analysis, will also influence krill dynamics throughout the sequence  
174 from spawning, through larval stages to the >5-year post-larval life.

175 While the weight of evidence above suggests a predominantly bottom-up control on krill  
176 that has caused a contraction in its distribution, the relative strength of top-down and bottom up  
177 factors will likely be scale-dependent. At small scales, predation can drive risk-reward trade-offs  
178 such as schooling behaviour and vertical migrations<sup>25</sup>. Over the much longer timespan of  
179 changing predator populations, the extent and sources of top-down control will vary<sup>1-3</sup>. Indeed,  
180 total density has not declined so rapidly as recruit density (**Extended Data Fig 1**). One possible  
181 explanation is a counteracting increase in post-larval survival, due to long-term changes in  
182 predation, increasingly relaxed intra-specific competition<sup>26</sup> or other density-dependent factors<sup>18</sup>.

183 The changes in density, mean size and range have a series of profound implications for  
184 krill (**Extended data Fig. 2**). First, the distribution is contracting into a diminishing area, because  
185 the meridians converge rapidly at high latitudes and further retreat is blocked by the continent  
186 itself. Since total abundance is a product of numerical density and area, reductions in numerical  
187 density will translate to greater reductions in total abundance<sup>2</sup>. Population genetics studies  
188 suggest major fluctuations in krill population size over longer timescales<sup>27</sup>, perhaps reflecting  
189 expansions and contractions from habitat refugia during glacial and inter-glacial epochs<sup>28</sup>. The  
190 highest krill densities tend to occur in shelf habitats<sup>12</sup> so the greater area of shelf in the south  
191 would result in an increasingly shelf-oriented population during warm periods. In a warmer  
192 world, a more fragmented, shelf-based distribution may restrict access to the deep water

193 needed for spawning and limit dispersal and basin-scale connection within the Antarctic  
194 Circumpolar Current<sup>22,29</sup>. The primary production in alternative, high latitude spawning areas  
195 might increase in future, but projections suggest that these areas will become more spatially  
196 restricted<sup>29</sup>, have a shorter growing season, and become adversely affected by ocean  
197 acidification effects on egg hatch success<sup>30</sup>.

198 Such changes in krill dynamics would have major ramifications for food web linkages and  
199 biogeochemical cycling (**Extended data Fig. 2**). When high densities of krill extend across the  
200 SW Atlantic sector, they support a suite of predators<sup>3,18</sup>. The fecal pellets cascading from krill  
201 schools provide pulses of carbon that can dominate particle export<sup>7</sup>. Their feeding and digestion  
202 also mobilises iron from diatoms and lithogenic sediment, in turn helping to fertilise  
203 phytoplankton blooms<sup>8,25</sup>. In a reorganised food web structure with a contracted distribution of  
204 larger krill over high latitude shelves, these functions will change. For example, the increased  
205 krill size might alter predator-prey interactions and allow greater swimming speeds, with the  
206 potential to migrate to cooler feeding grounds near the seabed<sup>25</sup>. This has major implications for  
207 nutrient cycles<sup>1,8</sup>, and could link krill to a different suite of predators<sup>25</sup>

208 Given the implications for food security and biodiversity, there is intense interest in  
209 projecting future stock sizes of krill, anchovies, sardines and other keystone species<sup>3,18,24</sup>.  
210 Current management of the krill fishery sets conservative catch limits but does not yet account  
211 for trends in stock size or distribution<sup>22</sup>. Models point to an ongoing increase in positive SAM  
212 anomalies for the next 50 years<sup>19</sup>, coupled with warming and reduced ice cover. This would  
213 suggest a further contraction in krill distribution, associated with a suite of mainly adverse effects  
214 (**Extended data Fig. 2**). However, climate-population relationships are inherently non-linear and  
215 can change abruptly as food webs shift into new states<sup>2</sup>. For example, abrupt latitudinal  
216 changes in bathymetry may constrain readjustments of distribution in polar regions, and  
217 **Extended Data Fig. 1** suggests that survival might be increasing, partially compensating for the  
218 sharp decline in recruitment. Species vary greatly in the extent to which their distributions  
219 change<sup>10</sup>, these responses being modulated by genetic adaptation or via adjustments to  
220 phenology or behaviour<sup>3,4</sup>. Various projections for krill have been made<sup>9,16,18,29,30</sup>, but given the  
221 likelihood of non-linearities<sup>18</sup>, these remain uncertain. Long time series thus remain the lifeblood  
222 of our understanding of climate change responses, so it is imperative that these are preserved.  
223 Doing so will allow the level of understanding needed for informed management decisions in  
224 rapidly changing polar ecosystems<sup>2,3</sup>.

225  
226

227 1 Smetacek, V. & Nicol, S. Polar ocean ecosystems in a changing world. *Nature* **437**, 362-368  
228 (2005).

229  
230 2 McBride M.M., Dalpadado, P., Drinkwater, K.F., Godø, O.R., Hobday, A.J., Hollowed, A.B.,  
231 Kristiansen, T., Murphy, E.J., Ressler, P.H., Subbey, S., Hofmann, E.E. & Loeng, H. Krill,

- 232 climate, and contrasting future scenarios for Arctic and Antarctic fisheries. *ICES J. Mar. Sci.* **71**,  
233 1934-1955 (2014).  
234
- 235 3 Constable, A.J. et al. Climate change and Southern Ocean ecosystems I: how changes in  
236 physical habitats directly affect marine biota. *Glob. Change Biol.* **20**, 3004-3025 (2014).  
237
- 238 4 Tarling, G.A., Ward, P. & Thorpe, S.E. Spatial distributions of Southern Ocean  
239 mesozooplankton communities have been resilient to long-term surface warming. *Glob. Change*  
240 *Biol.* doi: 10.11111/gcb.13834. (2017).  
241
- 242 5 Steinberg, D.K., Ruck, K.E., Gleiber, M.R., Garzio, L.M, Cope J.S., Bernard, K.S.,  
243 Stammerjohn, S.E., Schofield, O.M.E., Quetin, L.B. & Ross, R.M. Long term (1993-2013)  
244 changes in macrozooplankton off the Western Antarctic Peninsula. *Deep-Sea Res. I* **101**, 54-70  
245 (2015)  
246
- 247 6 Forcada, J. & Hoffman J.I. Climate change selects for heterozygosity in a declining fur seal  
248 population. *Nature* **511**, 462-465 (2014).  
249
- 250 7 Gleiber, M.R., Steinberg, D.K. & Ducklow, H.W. Time series of vertical flux of zooplankton  
251 fecal pellets on the continental shelf of the western Antarctic Peninsula. *Mar. Ecol. Prog. Ser.*  
252 **471**, 23-36 (2012).  
253
- 254 8 Schmidt, K, Schlosser, C., Atkinson, A., Fielding, S., Venables, H.J., Waluda, C.M. &  
255 Achterberg, E.P. Zooplankton gut passage mobilises lithogenic iron for ocean productivity. *Curr.*  
256 *Biol.* **26**, 2667-2673 (2016).  
257
- 258 9 Wiedenmann, J., Cresswell, K. & Mangel, M. 2008. Temperature- dependent growth of  
259 Antarctic krill: predictions for a changing climate from a cohort model. *Mar. Ecol. Prog. Ser.* **358**,  
260 191-202 (2008).  
261
- 262 10 Chen I.-C., Hill, J.K., Ohlemüller, R., Roy, D.B. & Thomas, C.D. Rapid range shifts of species  
263 associated with high levels of climate warming. *Science* **333**, 1024-1026 (2011).  
264
- 265 11. Atkinson, A., Siegel, V., Pakhomov, E.A, & Rothery, P. Long-term decline in krill stock and  
266 increase in salps within the Southern Ocean. *Nature* **432**, 100-103 (2004).  
267
- 268 12 Siegel, V. & Watkins, J.L. Distribution, biomass and demography of Antarctic krill, *Euphausia*  
269 *superba*. In Siegel V (ed) Biology and ecology of Antarctic krill. *Advances in Polar Ecology*.  
270 Springer, Switzerland, pp 21-100 (2016).  
271
- 272 13 Whitehouse, M.J., Meredith, M.P., Rothery, P., Atkinson, A., Ward, P. & Korb, R.E. Rapid  
273 warming of the ocean around South Georgia, Southern Ocean, during the 20<sup>th</sup> century: forcings,  
274 characteristics and implications for lower trophic levels. *Deep-Sea Res I* **55**, 1218-1228 (2008).  
275
- 276 14 Daufresne, M., Lengfellner, K., & Somner, U. Global warming benefits the small in aquatic  
277 ecosystems. *Proc. Natl. Acad. Sci.* **106**, 2788-12793 (2009).  
278
- 279 15 Loeb, V. et al. Effects of sea-ice extent and krill or salp dominance on the Antarctic food web.  
280 *Nature* **387**, 897-900 (1997).  
281
- 282 16 Quetin, L.B., Ross, R.M., Fritsen, C.H. & Vernet, M. Ecological responses of Antarctic krill to  
283 environmental variability: can we predict the future? *Antarctic Sci.* **19**, 253-266 (2007).  
284
- 285 17 Meyer, B. et al. The winter pack-ice zone provides a sheltered but food-poor habitat for larval  
286 Antarctic krill. *Nature Ecology and Evolution* <https://doi.org/10.1038/s41559-017-0368-3> (2017).  
287

- 288 18 Murphy, E.J., Trathan, P.N., Watkins, J.L., Reid, K., Meredith, M.P., Forcada, J., Thorpe,  
289 S.E., Johnston, N.M., Rothery, P. Climatically driven fluctuations in Southern Ocean  
290 ecosystems. *Proc Roy Soc B* **274**, 3057-3067 (2007).  
291
- 292 19 Bintanja, R, van Oldenborgh, G.J., Drifhout, S.S., Wouters, B. & Katsman, C. A. Important  
293 role for ocean warming and increased ice-shelf melt in Antarctic sea ice expansion. *Nature*  
294 *Geoscience* **6**, 376-379 (2013)  
295
- 296 20 Gillett, N.P. & Fyfe, J.C. Annular mode changes in the CMIP5 simulations. *Geophys. Res.*  
297 *Letts.* **40**, 1189-1193 (2013).  
298
- 299 21 Montes-Hugo, M., Doney, S.C., Ducklow, H.W., Fraser, W., Martinson, D., Stammerjohn,  
300 S.E., & Schofield, O. Recent changes in phytoplankton communities associated with rapid  
301 regional climate change along the western Antarctic Peninsula. *Science* **323**, 1470-1473 (2009).  
302
- 303 22 Nicol, S. Foster, J. & Kawaguchi S. The fishery for Antarctic krill – recent developments. *Fish*  
304 *Fisheries* **13**, 30-40 (2012).  
305
- 306 23 Cox, M.J., Candy, S., de la Mare, W.K., Nicol, S., Kawaguchi, S., & Gales, N. No evidence  
307 for a decline in the density of Antarctic krill *Euphausia superba* Dana, 1850, in the Southwest  
308 Atlantic sector between 1976 and 2016. *J. Crust. Biol.* (2018) doi:10.1093/jcbiol/ruy072.  
309
- 310 24 Hofmann, E.E. & Murphy, E.J. Advection, krill, and Antarctic marine ecosystems. *Ant. Sci.*  
311 **16**,487-499 (2004)  
312
- 313 25 Schmidt, K., et al. Seabed foraging by Antarctic krill: implications for stock assessment,  
314 benthic-pelagic coupling, and the vertical transfer of iron. *Limnol. Oceanogr.* **56**, 1411-1428.  
315 (2011).  
316
- 317 26 Ryabov, A.B., de Roos, A.M., Meyer, B., Kawaguchi, S. & Blasius, B. Competition-induced  
318 starvation drives large-scale population cycles in Antarctic krill. *Nature Ecol. Evol.* **1**, 0177  
319 doi:10.1038/s41559-017-0177(2017).  
320
- 321 27. Zane, L., Ostellari, L., Maccatrozzo, L., Bargalloni, L., Battaglia, B., & Patarnello, T.  
322 Molecular evidence for genetic subdivision of Antarctic krill (*Euphausia superba* Dana)  
323 populations. *Proc. Roy. Soc. Lond. B* **265**, 2387-2391 (1998)  
324
- 325 28 Spiridonov, V.A. A scenario of the late-Pleistocene-Holocene changes in the distributional  
326 range of Antarctic krill (*Euphausia superba*). *Mar. Ecol.* **17**, 519-541 (1996).  
327
- 328 29 Piñones, A. & Fedorov, A.V. Projected changes of Antarctic krill habitat by the end of the 21<sup>st</sup>  
329 century. *Geophys. Res. Letts.* **43**, 8580-8589 (2016).  
330
- 331 30 Kawaguchi, S., Ishida, A., King, R., Raymond, B., Waller, N., Constable, A., Nicol, S.,  
332 Wakita, M. & Ishimatsu, A. Risk maps for Antarctic krill under projected Southern Ocean  
333 acidification. *Nature Clim. Change* **3**, 843-847 (2013).  
334

### 335 **Author Contributions**

336

337 AA and SH contributed equally as first authors in providing the initial concept and analysis. AA,  
338 VS, EP: initial concept and construction of KRILLBASE databases; AA, EP, VS, CR, VL, DS,  
339 GT: supply of data to KRILLBASE; LG; mapping; SH: statistical analyses; ALL: Input of ideas to  
340 the study and to the manuscript.



341  
342  
343  
344  
345  
346  
347  
348  
349  
350  
351  
352  
353  
354  
355  
356  
357  
358  
359  
360  
361  
362  
363  
364  
365  
366  
367  
368  
369  
370  
371  
372  
373  
374  
375  
376  
377

**Acknowledgements.**

We thank all those who have supplied their data to KRILLBASE, especially Arthur Baker for help with locating old “Discovery” logbooks, and Roger Hewitt, Robin Ross, Langdon Quetin and So Kawaguchi for provision of data or scientific advice. Mark Jessopp, Helen Peat and Natalie Ensor helped with compiling and checking the databases, Gareth Marshall advised on SAM indices, Frances Perry helped with mapping, Dawn Ashby helped with the infographic figure and comments from George Watters and five anonymous reviewers improved the manuscript. SH was supported by Natural Environment Research Council (NERC) core funding to the BAS Ecosystems programme. AA and SS were funded through. AA and SS were funded through NERC’ National Capability modelling and Long-term Single Centre Science Programme, Climate Linked Atlantic Sector Science, grant number NE/R015953/1, and is a contribution to Theme 1.3 - Biological Dynamics. DKS was supported by the U.S. National Science Foundation’s Antarctic Organisms and Ecosystems Program (grant PLR 1440435).

**Competing Interests: none**

378 **Table 1. Significant relationships among krill density, mean length, Southern Annular**  
 379 **Mode and year.**

Model	Fixed effects model	m1 (P)	m2 (P)	c1	c2	N	R <sup>2</sup> <sub>m</sub>	R <sup>2</sup> <sub>c</sub> (AIC)
1	DENSITY = (m1+m2*LAT)*YEAR+c1+c2*LAT	-0.065 (<0.001)	0.044 (<0.001)	131	-87	290	0.08	0.15 (773)
2	LENGTH = m1*YEAR+c1	0.173 (<0.001)		-305		146	0.04	0.33 (931)
3	RECRUIT DENSITY = m1*YEAR+c1	-0.069 (<0.001)		137		124	0.08	0.10 (426)
4	D.DENSITY = m1*D.LENGTH+c1	-0.044 (<0.001)		0.138		124	0.01	0.01 (283)
5	D.DENSITY = (m1+m2*SHELF)*D.SAM+c1	-0.229 (<0.001)	0.577 (<0.05)	-0.186		290	0.01	0.02 (768)
6	D.LENGTH = m1*D.SAM+c1	2.197 (<0.01)		0.093		146	0.03	0.38 (918)
7	D.RECRUIT DENSITY = m1*D.SAM+c1	-0.352 (<0.05)		-0.024		115	0.01	0.03 (417)

380  
 381  
 382 Linear mixed model results indicating significant time trends in Log<sub>10</sub> standardised krill density,  
 383 no. m<sup>-2</sup> (model 1), mean length in mm (2), and Log<sub>10</sub> density of recruits, no. m<sup>-2</sup> (3); covariance  
 384 in length and density (4); and relationships between the Southern Annular Mode index and  
 385 each of standardised krill density (5), mean length (6) and density of recruits (7). The fixed  
 386 effects are expressed in terms of the coefficients m1, m2, c1 and c2. N is the number of  
 387 observations (these are plotted in [Fig. 2](#)). All models include random spatial unit effects.  
 388 Models 2 and 6 also include random year effects. R<sup>2</sup><sub>m</sub> is the marginal pseudo-R<sup>2</sup> indicating  
 389 variance explained by the fixed effects and R<sup>2</sup><sub>c</sub> is the conditional pseudo-R<sup>2</sup> indicating variance  
 390 explained by both fixed and random effects. AIC is the Akaike information criterion. Variables  
 391 prefixed “D” were de-trended. LAT values 0 and 1 represent latitudes north and south of 60°S  
 392 respectively and SHELF values 0 and 1 represent shelf (≤1000m depth) and oceanic waters  
 393 respectively.

394  
 395

396  
397  
398  
399  
400  
401  
402  
403  
404  
405  
406  
407  
408  
409  
410  
411  
412  
413  
414  
415  
416  
417  
418  
419  
420  
421  
422  
423  
424  
425  
426  
427  
428  
429  
430  
431  
432

**Figure 1 (caption on next page)**

**Fig. 1. Southward contraction of krill distribution within the SW Atlantic sector.**

**a** Kernel analysis visualising hotspots of krill density in the SW Atlantic sector during the *Discovery* sampling era (1926-1939) and the first and second halves of the modern era, based on the area sampled heavily across all three periods (see **Methods and Fig S1**). Blue isobaths denote the 1000m boundary between shelf and oceanic habitats. Within each map, the kernel analysis identifies relative hotspot areas of high density, signified by intensity of red shading. For a quantitative analysis the histograms denote the mean density of krill in six comparable 2.5° latitude bands with > 50 stations sampled in each era (see **Methods**). Note changes in scale between each of the three eras. Thick blue lines across maps and histograms indicate the centre of krill density (i.e. density-weighted mean latitude; see **Methods**). **b** Trends in log<sub>10</sub>-transformed mean standardised krill density north and south of 60°S. Small points represent the densities in underlying records, large dots represent the annual means of these data, weighted by the number of stations per record. Pink dots represent seasons with <50 stations (average 27 compared to an overall average of 123 stations per season). Solid blue trend lines were fitted using simple linear regression ( $P < 0.001$ ,  $< 0.01$  adjusted  $R^2 = 0.52, 0.22$  for North and South respectively). Linear mixed model no.1 in **Table 1** and in **Supplementary Table 1** provides statistical support for these trends and the significantly greater decline in the North. **Fig. 2** provides finer latitudinal resolution, for instance showing an increase in density in the far south

433  
434  
435  
436  
437  
438  
439  
440  
441  
442  
443  
444  
445  
446  
447  
448  
449  
450  
451  
452  
453  
454  
455  
456  
457  
458  
459  
460  
461  
462  
463  
464  
465  
466  
467  
468  
469  
470  
471  
472  
473  
474  
475  
476  
477  
478  
479

480 **Fig. 2 A latitudinal gradation of change in krill dynamics over the last 40 years.** The points are  
481 the spatio-temporal means that are included in the linear mixed model analysis in Table 1. These are  
482 grouped by latitude (2.5° band) and bathymetry (shelf  $\leq 1000\text{m}$  water depth, versus oceanic waters).  
483 LOESS curves indicate trends within each spatial unit. The particularly well sampled bands at South  
484 Georgia and near the tip of the Antarctic Peninsula (**Figure S2**) are labelled for reference. **a** Density  
485 of total post-larvae (i.e. new recruits plus older krill) from 7625 stations. Evidence for a range  
486 contraction is the sharp decline in density at the northern range fringes, with a progressive

487 stabilisation and then reversal of the trends towards the south. **b** Data from 4308 length frequency  
 488 sampling stations showing spatially-consistent increases in mean length. **c** Recruit density has  
 489 declined very abruptly over the last 40 years in all areas except possibly for the far south. This is  
 490 reflected both in the increase in mean length and the decline in density of total post-larvae. These  
 491 trends appear broadly congruent across both shelf and oceanic habitats.

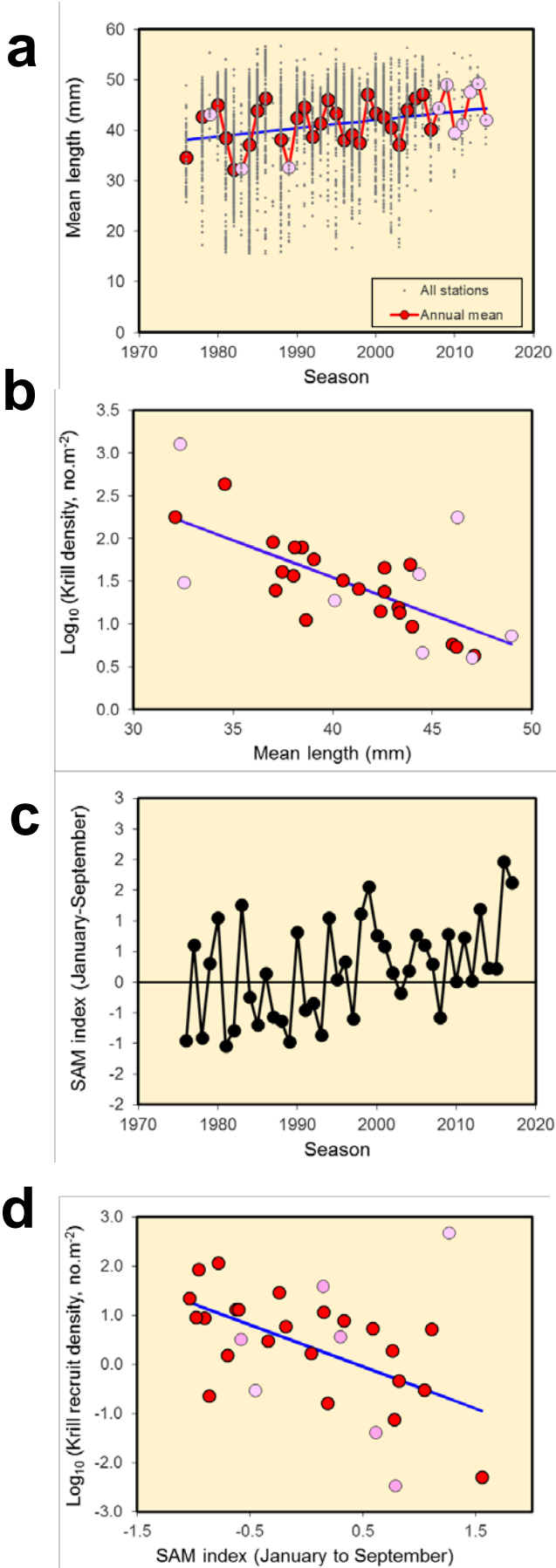


**Fig. 3. Climatic forcing provides one mechanism for an increase in mean krill length and declines in recruitment and density.**

The linear mixed model results in **Table 1**, which include de-trending where appropriate, provide statistical support for the simple linear regression relationships illustrated here. **a**

Increase in mean length of krill. Regression  $P < 0.05$ , adjusted  $R^2 = 0.09$ ; see mixed model no. 2 in **Table 1**. Small points represent the mean lengths in underlying records. Pink dots represent seasons with  $< 50$  stations (average 18 compared to an overall average of 116 stations per season). **b** Relationship between density and mean length.

Regression  $P < 0.001$ , adjusted  $R^2 = 0.47$ ; for de-trended data see mixed model no. 4 in **Table 1**. **c** Inter-annual variation in January-September SAM anomaly during the modern era. Data are plotted with a 1-year lag, (i.e. Jan-Sept 2015 anomaly is plotted as 2016). **d**. Relationship between mean density of new recruits (density of individuals  $< 30$  mm long) and the SAM anomaly in the January-September period preceding the krill sampling season.

Regression  $P < 0.001$ , adjusted  $R^2 = 0.30$ . Mixed model nos. 5 to 7 in **Table 1** provide relationships between krill and SAM. Pink dots represent seasons with  $< 50$  stations for either length or density.

526  
527  
528  
529  
530  
531  
532  
533  
534  
535  
536  
537  
538  
539  
540  
541  
542  
543  
544  
545  
546  
547  
548  
549  
550  
551  
552  
553  
554  
555  
556  
557  
558  
559  
560  
561  
562

**Extended data Fig. 1. Recruit density has declined more rapidly than total post-larval density, which may be due to an increase in survival of older krill.** Linear mixed models of  $\log_{10}$ (mean density of new recruits) and  $\log_{10}$ (mean total post-larval density) versus year confirm that the trend in the former (-0.070) is significantly ( $P < 0.001$ ) more negative than the trend in the latter (-0.042) over the comparable joint measurement period. This difference is illustrated with simple linear regressions (blue lines) fitted to annual means of **a** mean recruit density ( $P < 0.001$ , adjusted  $R^2 = 0.39$ ) and **b** mean total post-larval density ( $P < 0.001$ , adjusted  $R^2 = 0.499$ ). Pink dots represent seasons with  $< 50$  stations.

**Extended data Fig. 2. Ramifications of a changing abundance, distribution and body size of krill.** The illustration portrays a view looking north-eastwards along the Antarctic Peninsula, AP towards South Georgia, SG (i.e. from bottom left corner of Fig. 1a), with the intensity of red shading showing changes in krill density and distribution that we have found. For reference, seasonal mean water temperatures at South Georgia have risen by  $1.6^\circ\text{C}$  over the last  $\sim 80$  years<sup>13</sup>. We have summarised the potential implications of ongoing and future climate change this century (right hand panel) based on the observed changes and the projected increase in positive SAM anomalies for the next  $\sim 50$  years<sup>20</sup> The schematic is not intended to be to scale but for reference is intended to span from  $\sim 70^\circ\text{S}$  up to  $\sim 50^\circ\text{S}$ ; this represents roughly a doubling of maximum potential habitat areas between any pair of longitudes.

**Methods (text references are listed at the end of the Methods)**

563

## 564 **1. KRILLBASE abundance database**

565 We have created a database, entitled “KRILLBASE-abundance<sup>31</sup>”, to rescue and  
566 collate all available data from untargeted net catches across the Southern Ocean. It was  
567 compiled through “data rescue” from old notebooks, the authors’ datasets, published reports  
568 and submissions by other data contributors. The full database comprises 15,194 net hauls  
569 spanning the 1926 – 2016 period and has data on the numerical density (number m<sup>-2</sup>) of  
570 postlarval *Euphausia superba*. This dataset (**Fig S2**) is derived from stations at predetermined  
571 or randomly selected positions and excludes hauls targeted on krill schools. It includes ~50%  
572 more data than previously published versions of the database<sup>11,32</sup>. The full database is  
573 circumpolar and comprises data from 10 nations spanning 56 sampling seasons. Section 13  
574 describes data availability.

575

## 576 **2. KRILLBASE length-frequency data base.**

577 We have compiled a separate database, entitled “KRILLBASE-length frequency”,  
578 which includes length, sex and maturity-stage data for *Euphausia superba*. Unlike the  
579 abundance counterpart, this contains data from hauls targeted on krill schools as well as those  
580 from random or predetermined locations. This database is also circumpolar, comprising over  
581 11,000 sampling stations over 47 seasons within the period 1926-2014 (**Fig. S2a**). With over 1  
582 million individual krill length measurements both from scientific and commercial nets, the  
583 length-frequency database is much larger than, and compiled independently from, the  
584 abundance database<sup>33</sup>. The full dataset comprises data from 10 nations, either available in the  
585 authors’ home institutes, sent directly by other contributors or transcribed from publications  
586 and reports. Section 13 describes data availability.

587

## 588 **3. Transformation and screening of data**

589 KRILLBASE-abundance data are in units of numbers of postlarval krill m<sup>-2</sup>, hereafter  
590 described simply as “density”. Both this and the length-frequency database required some  
591 screening for the current analyses. The SW Atlantic sector of interest was defined as 20°-  
592 80°W and between the Antarctic Polar Front and 75°S. We divided hauls according to “austral  
593 summer” season (for example the 1985 season encompassed all stations sampled between 1  
594 Oct 1984 and 30 April 1985), thereby screening out winter data. Most sampling in both  
595 screened datasets was in the summer months, with 76% of hauls in the period December to  
596 February. For consistency with other work<sup>32</sup>, the krill-density data were further screened  
597 according to the net sampling depths, removing all hauls where the upper sampling depth was  
598 > 20m or the lower sampling depth was < 50m. The median upper and lower depths were 0  
599 and 170 m respectively in the screened density dataset. The length frequency dataset was

600 screened by removing all krill < 15mm long, since these include larvae. Nets with large  
601 meshes provide biased estimates of size distribution, therefore we excluded data from all  
602 commercial or semi-commercial trawls and scientific nets with meshes > 6 mm (e.g.,  
603 RMT25's).

604 We have included both targeted and non-targeted hauls for analysis of length  
605 frequency distribution, following the recommendation<sup>34</sup> that the priority is to sample a sufficient  
606 number of krill to be representative of the wider population, which can require combining  
607 targeted and non-targeted hauls where necessary. However to test whether this may have  
608 caused a bias in the time trends we divided the hauls into those that provided a representative  
609 sample of the whole top 100m layer and the remainder (including targeted hauls). An increase  
610 in mean krill length was seen independently in both subsets of data, supporting [Fig. 2](#) and [3](#).  
611 Therefore we simply pooled the two data sources for subsequent analyses.

612 The krill-density estimates were based on a wide range of sampling net types, depth  
613 ranges and times of year, all of which can potentially bias temporal-spatial trends. We  
614 therefore applied conversion factors to each haul to standardise to a single, relatively efficient  
615 net sampling method. The chosen efficient sampling combination was a night-time haul with  
616 an 8 m<sup>2</sup> net from 0-200 m on 1 January. The statistical method of adjusting the krill density  
617 values to this sampling method is previously described<sup>31,32</sup>.

618 It is important to note that this standardisation model only used nets sampled  
619 concurrently within the modern era; we could not use the 1 m diameter nets with release gear  
620 used during the *Discovery* era (1920s and 1930s) for the standardisation as there were no  
621 other net types fished concurrently. Therefore the absolute values of standardised krill density  
622 presented for the *Discovery* era (top panels of [Fig 1a](#)) must be considered as approximate.  
623 Nevertheless, and particularly for the modern era, we believe that this data standardisation  
624 provides a more consistent view of spatial-temporal changes in krill density than the raw  
625 density data. Therefore for all analyses in the main text we used standardised densities. Un-  
626 standardised data as well as subsets of the data according to sampling method were analysed  
627 to assess whether the results were broadly coherent and not sensitive to the method used  
628 ([see Supplementary Table 1](#)).

629

#### 630 **4. Environmental data**

631 The KRILLBASE-abundance database includes data on depth at each sampling  
632 station, based on a mean value for a 10 km radius buffer around each station from the GEBCO  
633 bathymetry<sup>31</sup>. These values provide a basis for characterising whether the station was over  
634 the shelf ( $\leq 1000\text{m}$ ) or in oceanic waters ( $> 1000\text{m}$ ). We tested krill indices against a variety of  
635 physical variables (see Methods section 9). These included first, the Southern Annular Mode  
636 anomalies, obtained from the British Antarctic Survey, Natural Environment Research



637 Council<sup>35</sup> (<http://www.nerc-bas.ac.uk/icd/gjma/sam.html>). Multivariate ENSO (MEI) values  
638 were obtained from the National Oceanic and Atmospheric Administration, Earth System  
639 Research Laboratory, Physical Sciences Division<sup>36</sup>  
640 <https://www.esrl.noaa.gov/psd/data/correlation/mei.data>.

641 For sea-ice, median values of ice cover were obtained from two passive microwave  
642 radiometer datasets; the Microwave Scanning Radiometer-Earth Observation System (AMSR-  
643 E)<sup>37</sup> aboard the NASA's Aqua satellite and the Defense Meteorological Satellite Program SSM/I  
644 <http://nsidc.org/data/nsidc-0051.html>. From these, the northern latitudes of 15% concentration  
645 were obtained. In addition we tested indices of fast ice timing of formation, breakout and  
646 duration from the South Orkney Islands time series<sup>38</sup>.

647

## 648 **5. KRILLBASE data coverage and spatial-temporal pooling**

649

650 Because KRILLBASE is a data rescue and compilation project, data from the  
651 abundance and length frequency databases were not distributed homogeneously in time and  
652 space. To counteract this we have used a suite of methods and sampling units to examine key  
653 relationships. Spatially these include division of the SW Atlantic sector (20°-80°W) data into  
654 2.5° latitudinal bands, and into shelf versus oceanic portions. This resulted in 12 spatial units  
655 defined by 2.5° latitudinal band and bathymetry (shelf versus oceanic waters). Following  
656 reference<sup>2</sup> we excluded spatial units with fewer than 50 stations or 5 sampling seasons from  
657 the spatial visualisations in **Fig. 1a** and **Fig S2**. Temporally we have used austral "year" (i.e.  
658 from October of the previous year to April in the given year) as the basic unit of sampling,  
659 based on the great variability in krill density and mean length observed between successive  
660 years due to inter-annual variation in recruitment<sup>15,18,,26,39-41</sup>. Our analyses (e.g. **Figs. 1b, 2,**  
661 **S1**) provide time trends and relationships that were broadly coherent right across the SW  
662 Atlantic sector. For this reason, our illustration of key relationships in **Fig. 3** is at this whole-  
663 sector scale, supported by the mixed models that include the finer subdivisions described  
664 above.

665

## 666 **6. Visualisation of the contraction in distribution**

667 To provide a visualisation of the changes in distribution revealed statistically by the  
668 mixed model no.1 (**Table 1**) we have divided the sampling into 3 periods based on sequential  
669 years of sampling (namely the *Discovery* era of the 1920s and 1930s, then further dividing the  
670 modern era, 1976-2016, into two roughly equal time spans). Sample coverage in each period  
671 is provided in **Fig S2**. We further restricted the analysis to an area sampled adequately in all  
672 three eras. This was defined by a polygon (red line in **Fig S2**) including a sub-region that was  
673 sampled consistently but in lower density (hatched area in **Fig S2**). To visualise changes in  
674 the hotspots of krill density (**Fig 1a**) we used the kernel density tool in ArcGIS to grid the

675 density sample points from each sampling era. Kernel density estimation is a non-parametric  
676 smoothing interpolation that calculates the density of points in a specified distance around  
677 each feature. We used this approach because it is not prone to edge effects and, across the  
678 domain of each map, could objectively identify hotspot areas of elevated density.

679

## 680 **7. Calculation of population central latitude in each era**

681 We calculated the population central latitude in each era based on the stratification  
682 procedure of six 2.5° latitudinal bands described in section 5 above, and illustrated in **Fig 1a**.  
683 Population central latitude is the sum of the products of stratum mean density and stratum mid  
684 latitude, divided by the sum of stratum mean densities. While the substantial southwards  
685 contraction of range within the modern era (**Fig. 1a**) is supported independently by both shelf  
686 and oceanic krill sampling stations, we should stress that this analysis, plus the spatial  
687 depictions in **Fig1a** are for illustrative purposes only. Statistical evidence for a range  
688 contraction is provided by the spatio-temporal analysis within mixed model no. 1 in **Table 1**  
689 (see also section 10 below).

## 690 **8. Calculation of recruit density**

691 Recruit density is defined here as the mean density of postlarval krill  $\leq 30$  mm in  
692 length<sup>40</sup>. This is an estimation of the density of post-larval krill that are likely to be about 1 year  
693 old within the October to April timeframe of each year's observations<sup>40</sup>. Density of new recruits  
694 in each season was thus calculated as a product of proportional recruitment (the fraction of  
695 the krill measured that were 15-30 mm in length) and the mean density of all postlarvae.

696

## 697 **9. Preliminary analysis of relationships with environmental variables.**

698 In a series of preliminary analyses we analysed inter-annual variability in a series of  
699 response variables, namely total post-larval krill density, density of recruits and mean length at  
700 a range of spatial and temporal scales. The candidate explanatory variables included winter  
701 sea-ice cover (indexed by ice formation, duration, and breakout times from the South Orkneys  
702 fast ice dataset<sup>38</sup>) plus satellite-derived monthly extents of 15% ice northerly extent averaged  
703 within a series of 10° longitude bands. Climatic indices included SAM (Southern Annular  
704 Mode) and MEI (multivariate El Niño/Southern Oscillation) monthly data with variable lags and  
705 integration periods. The best fit Gaussian GLM (weighted by the number of krill sampling  
706 stations per year) had SAM as the explanatory variable (i.e. average of monthly SAM  
707 anomalies for the period January to September preceding the October to April season of the  
708 krill observations) . At the large scales of our study, the best sea-ice relationship explained  
709 much less of the variance than SAM, perhaps reflecting more localised specific conditions of  
710 ice-krill relationships<sup>16,40,41</sup>. ENSO has also been identified as a driver of krill dynamics near  
711 the Antarctic Peninsula<sup>39-41</sup>. We found that ENSO (indexed by the MEI) related significantly to

712 krill with very short and long lag times, but these disappeared when added to models  
713 alongside SAM, which was thus by far the clearest predictor at the whole SW Atlantic scale.

714

## 715 **10. Preliminary analysis of trends**

716 We used LOESS regression, implemented using the loess function in the R package  
717 stats<sup>43</sup> (span=1, degree=1) to visualise time trends in response variables: These were across-  
718 station averages of numerical density, length, and recruit density, grouped by season and  
719 spatial unit. The spatial units were defined by latitude (2.5° bands) and bathymetry (shelf  
720 versus oceanic waters >1000m deep) (Fig. 2). Numerical density and recruit density were  
721 increased by a constant (half of the minimum numerical density across all spatio-temporal  
722 units) and log<sub>10</sub> transformed prior to analysis.

723 Encounter probability (the proportion of samples in which the subject species is  
724 present) is a common metric of species distribution. This metric (Fig. S 1) corroborated our  
725 findings on numerical density (Fig. 2), namely a strong decline in the north, trending towards a  
726 more stable situation towards the south, suggestive of a contraction in the distribution.  
727 However, we chose the density results for our main analysis, given the highly heterogeneous  
728 distribution of krill.

729

730 .

## 731 **11. Linear mixed models**

732 The datasets used in this analysis were compiled from multiple surveys with a variety  
733 of designs, locations and sampling methods. Standardisation allows comparison of data from  
734 individual stations, but analysis of temporal patterns in such data must also ameliorate the  
735 effects of pseudoreplication and inhomogeneity of variance. Further issues include potential  
736 temporal autocorrelation and the risk of spurious correlation due to time trends in multiple  
737 variables. Our exploration of changes in krill population characteristics and their relationships  
738 with environmental variables in the modern era (1976 to 2016) addresses each of these  
739 issues.

740 To ameliorate the effects of pseudo-replication, our analysis was conducted using  
741 linear mixed models which considered spatial unit, year and the interaction between them, as  
742 random effects. We used the lme function in the R package nlme<sup>42</sup> to fit models using  
743 restricted maximum likelihood.

744 We investigated the fixed effects of latitude by including a candidate variable, LAT,  
745 indicating whether the sample was north and south of 60°S. This gave a reasonable balance  
746 of data between north and south but it was not possible to explore bathymetric contrasts in  
747 length and recruit density north of 60°S (Fig. 2). The main candidate explanatory variable was  
748 year for models 1-3 in Table 1, de-trended mean length for model 4 and de-trended SAM

749 (average of monthly anomalies for the period January to September preceding the krill  
750 sampling season) for models 5 to 7. We considered the most complete form of each model  
751 including fixed effects for the main candidate variable plus latitude and bathymetric bin where  
752 feasible; interactions between them; and random effects.

753 We arrived at the final models presented in [Table 1](#) by using model selection to  
754 identify fixed and random effect variables from the set of candidates listed above, including  
755 interactions. Model selection also identified appropriate representations of variance as a  
756 function of the reciprocal of the number of stations (from candidate fixed, power and  
757 exponential functions), to ameliorate the effects of inhomogeneity of variance. It also identified  
758 an appropriate correlation structure (from candidate autoregressive order 1 and  
759 autoregressive moving average functions) to ameliorate the effects of temporal autocorrelation  
760 where relevant. Model selection was based on AIC, except the identification of fixed effects,  
761 which also considered differences between models based on likelihood ratios. The selected  
762 variance function was a power function for all models except model 2, which used a linear  
763 function.

764 To avoid spurious correlations when both the response and main candidate  
765 explanatory variable included a time trend, we de-trended both variables using the relevant  
766 time trend model. The de-trended variable was the original value minus the fitted value based  
767 on fixed effects.

768 We used visual checks to verify that response data were approximately normally  
769 distributed and that model fits were convincing. We verified that the autocorrelation statistics in  
770 the selected models were not significantly different from zero. We also used the Levene test  
771 (R package `car`<sup>44</sup>) to verify that each model was not significantly affected by heteroscedacity.  
772 Finally, we used the `r.squaredGLMM` function in the R package `MuMIn`<sup>45</sup> to estimate the  
773 variance explained by the fixed and random effects in each model. In high variability datasets  
774 like ours, the variance explained by linear models featuring one or two explanatory variables is  
775 typically low, particularly when variables are detrended. The main statistic for detecting  
776 relationships is the P value, which indicates whether the linear model slope is significantly  
777 different from zero.

778 To assess the difference in time trends between recruit density and total post-larval  
779 density ([Extended data Fig 1](#)) we restricted the data set to years and spatial units for which  
780 both types of density estimate were available. We constructed a linear mixed model with  
781 density as the response variable, year as the main explanatory variable and an additional  
782 explanatory variable indicating the type of density estimate (recruit or total post-larval). A  
783 significant interaction between explanatory variables indicates a significant difference in slope.

784 We explored the sensitivity of the time trend in krill density to data selection and  
785 processing by fitting model 1 to alternative versions of the dataset ([Supplementary Table 1](#)).

786 Specifically, we used (i) unstandardised krill density data, (ii) data only from nets with nominal  
787 mouth areas  $>3\text{m}^2$ , and (iii) data only from nets with nominal mouth areas  $\leq 3\text{m}^2$ . All models  
788 identified the negative time trend, but the models fitted to smaller datasets filtered by net size  
789 did not identify a latitudinal difference in trend. As krill aggregate in dense swarms with few  
790 krill between, the probability of estimated density being zero increases at low sample sizes.  
791 Consequently, when averages based on  $<15$  stations are included, there is a weak  
792 relationship between number of stations and average density. To confirm that the variance  
793 function ameliorates this effect, we also fitted all models with density or recruit density as a  
794 response variable to restricted datasets which excluded averages based on  $<15$  stations. In all  
795 cases the main fixed effects remained significant.

796

## 797 **12. Calculated decline in density and biomass during the modern sampling era**

798

799 The average separation between sampling in the first and second halves (1976-1995 and  
800 1996-2016) of the modern era is 20.5 years. We thus used the time trends in **Table 1** to  
801 determine respective average changes in density and length over 20.5 years. We used the  
802 unweighted mean of the north and south slopes for density, so the estimated change is  
803 analogous to that expected for a transect with equal length on either side of latitude  $60^\circ\text{S}$ .  
804 Mean lengths were converted to individual dry mass using Scotia Sea-specific length-mass  
805 regressions<sup>46</sup> and biomass density was calculated as the product of individual dry mass and  
806 numerical density. These revealed the 70% decline in numerical density and 59% decline in  
807 biomass density quoted in the text.

808

## 809 **13. Data availability**

810 We have made the KRILLBASE abundance database publically available from the  
811 Polar Data Centre at the British Antarctic Survey <http://doi.org/brg8> with supporting metadata<sup>31</sup>  
812 which should be consulted for further details. Likewise KRILLBASE Length frequency data are  
813 also available on request to the Polar Data Centre, with supporting metadata.

814

815

816

### **Additional Method references**

817

818 **31.** Atkinson A. et al. KRILLBASE: a circumpolar database of Antarctic krill and salp numerical  
819 densities, 1926-2016. *Earth Syst. Sci. Data* **9**, 1-18 (2017).

820

821 **32.** Atkinson, A., Siegel, V., Pakhomov, E.A., Rothery, P., Loeb, V., Ross, R.M., Quetin, L.B.,  
822 Fretwell, P., Schmidt, K., Tarling, G.A., Murphy, E.J. & Fleming A. Oceanic circumpolar  
823 habitats of Antarctic krill. *Mar. Ecol. Prog. Ser.* **362**, 1-23 (2008).

824

825 **33.** Tarling, G.A., Hill, S., Peat, H., Fielding, S., Reiss, C. & Atkinson A. Growth and shrinkage  
826 in Antarctic krill *Euphausia superba* is sex-dependent. *Mar Ecol. Prog. Ser.* **547**, 61-78 (2016).

827

828 **34.** Watkins, J. Sampling krill. In: Everson, E. (ed). Krill biology, ecology and fisheries.  
829 Blackwell Science, Oxford, pp 8-39. (2000)

830

831 **35.** Marshall, G. J. Trends in the Southern Annular Mode from observations and  
832 re-analyses. *J. Clim.* **16**, 4134–4143 (2003).

833

834 **36.** Wolter, K. & Timlin, M. S. El Niño/Southern Oscillation behaviour since 1871  
835 as diagnosed in an extended multivariate ENSO index (MEI.ext). *Intl. J. Clim.*  
836 **31**, 1074–1087 (2011).

837

838 **37.** Spreen, G., Kaleschke, L. & Heygster, G. Sea ice remote sensing using AMSR-E 89-GHz  
839 channels. *J. Geophys Res-Oceans* **C02S03** (2008).

840

841 **38.** Murphy, E.J., Clarke, A., Abram, N.J. & Turner, J. Variability in sea ice in the northern  
842 Weddell Sea during the 20<sup>th</sup> century. *J. Geophys. Res.-Oceans* **119**, 4549-4572. (2014)

843

844 **39.** Ross, R.M., Quetin, L.B., Newberger, T., Shaw, C.T., Jones, J.L. Oakes, S.A. & Moore,  
845 K.J. Trends, cycles, interannual variability for three species west of the Antarctic Peninsula,  
846 1993-2008, *Mar. Ecol. Prog. Ser.* **515**, 11-32 (2014).

847

848 **40.** Saba G.K. et al. Winter and spring controls on the summer food web of the coastal West  
849 Antarctic Peninsula. *Nature Communications* **5**, 4318 doi 10.1038/ncomms5318 (2014).

850

851 **41.** Loeb, V. & Santora, J.A. Climate variability and spatiotemporal dynamics of five Southern  
852 Ocean krill species. *Prog. Oceanogr.* **134**, 93-122 (2015).

853

854 **42.** Pinheiro J, Bates D, DebRoy S, Sarkar D and R Core Team. *nlme: Linear and Nonlinear*  
855 *Mixed Effects Models*. R package version 3.1-131, <https://CRAN.R-project.org/package=nlme>  
856 (2017).

857

858 **43.** R Core Team. R: a language and environment for statistical computing. R Foundation for  
859 statistical computing, Vienn. ISBN 3-900051-07-0. <http://www.R-project.org/>. (2013).

860

861 **44.** Fox J. & Weisberg, S. An “R” Companion to applied regression. Second Edition. Thousand  
862 Oaks, California. <http://socserv.socsci.mcmaster.ca/jfox/Books/Companion> (2011).

863

864 **45.** Barton K. *MuMIn: Multi-model inference*. R package version 1.9.13. [http://CRAN.R-](http://CRAN.R-project.org/package=MuMIn)  
865 [project.org/package=MuMIn](http://CRAN.R-project.org/package=MuMIn) (2013)

866

867 **46.** Hill, S.L., Phillips, A. & Atkinson, A. Potential climate change effects on the habitat of  
868 Antarctic krill in the Weddell quadrant of the Southern Ocean. *PLoS One* **8** (8), e72246 (2013).

869

870

## 871 **SUPPLEMENTARY APPENDIX SECTION**

872

873

874

875

876

877

878

879

880

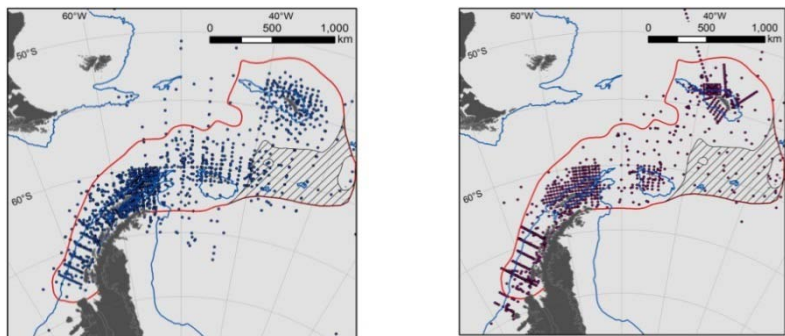
881  
882  
883  
884  
885  
886  
887  
888  
889  
890  
891  
892  
893  
894  
895  
896  
897  
898  
899  
900

**Fig. S1 Tends in krill encounter probability by latitude suggest a decline in krill presence north of 60°S.** Spatio-temporal means of encounter probability (proportion of hauls that contained krill), grouped by latitude (2.5° band) and bathymetry (shelf ≤1000m water depth, versus oceanic waters). LOESS curves indicate trends within each spatial unit.

**1926-1939**

**1976-1995**

**1996-2016**



906  
907  
908  
909  
910

**Fig. S2. Sample coverage within SW Atlantic sector showing coverage in each time period illustrated for krill density data.** The red line encloses the region with adequate sampling in all three periods, albeit with less consistent sampling density in the hatched



911 area. This red-encircled area was selected for visualisation of density hotspots with kernel  
 912 analysis.

913  
 914  
 915  
 916  
 917  
 918  
 919  
 920  
 921  
 922  
 923  
 924  
 925  
 926  
 927 **a**  
 928 **b**

929 **Fig. S3. Coverage and trends derived from the krill length frequency database in each**  
 930 **sampling period. a** Sample coverage in each period; points indicate stations. **b** For an initial  
 931 visualisation of changes in mean length across the three eras we divided the SW Atlantic sector  
 932 into a series of 5° latitude by 10° longitude grid cells. The region from 60-65°S was sampled more  
 933 intensively than any others, enabling its further division into finer, 2.5° latitudinal bands as done for  
 934 the linear mixed models. Mean krill lengths within each grid cell within each era were then  
 935 calculated. For an overview of changes in mean length across the three eras we used ocean data  
 936 view visualisations of those grid cells which had data in all three periods. Most grid cells  
 937 experienced an increase in mean length from the *Discovery* era through to the most recent  
 938 sampling period.  
 939  
 940

941 **Supplementary Table 1.**

942 **Results of linear mixed models fitted to alternative datasets to assess sensitivity to**  
 943 **data selection and standardisation of density data to a single net sampling method.**  
 944

Model*	Summary	m1 (P)	m2 (P)	c1	c2	N	R <sup>2</sup> <sub>m</sub>	R <sup>2</sup> <sub>c</sub> (AIC)
1	Unstandardised DENSITY ~ YEAR*LAT	-0.063 (<0.001)	0.048 (<0.001)	127	-95	290	0.07	0.13 (756)
1	Standardised DENSITY ~ YEAR*LAT (where net mouth<3m <sup>2</sup> )	-0.102 (<0.001)	0.057 (NS)	204	-112	60	0.18	0.18 (231)
1	Standardised DENSITY ~ YEAR*LAT	-0.034 (<0.01)	0.015 (NS)	69	-30	260	0.02	0.08 (640)

	(where net mouth $\geq 3m^2$ )							
Models fitted to data with at least 15 stations per density estimate								
1	Standardised DENSITY ~ YEAR*LAT	-0.071 (<0.001)	0.045 (<0.01)	144	-89	144	0.01	0.02 (318)
1	Unstandardised DENSITY ~ YEAR*LAT	-0.065 (<0.001)	0.045 (<0.01)	131	-90	144	0.01	0.01 (312)
1	Standardised DENSITY ~ YEAR*LAT (where net mouth<3m <sup>2</sup> )	-0.140 (<0.01)		280		21	0.00	0.00 (84)
1	Standardised DENSITY ~ YEAR*LAT (where net mouth $\geq 3m^2$ )	-0.026 (<0.001)		53		123	0.01	0.03 (238)
3	RECRUIT DENSITY ~ YEAR	-0.064 (<0.001)		127		88	0.05	0.05 (286)
4	D.DENSITY ~ D.LENGTH	-0.043 (<0.001)		0.209		88	0.00	0.00 (170)
5	D.DENSITY ~ D.SAM+SHELF	-0.236 (<0.05)	0.265 (NS)	0.226		144	0.00	0.00 (323)
7	D.R.DENSITY ~ D.SAM	-0.477 (<0.05)		-0.284		88	0.01	0.01 (274)

945  
946  
947  
948  
949  
950  
951

\* Number refers to the comparable model, fitted to all data, presented in [Table 1](#).  
Other details as [Table 1](#).